Shallow-Water Acoustic Communications Channel Modeling Using Three-Dimensional Gaussian Beams

Paul A. Baxley, Homer Bucker, Vincent K. McDonald, and Joseph A. Rice
SSC San Diego

Michael B. Porter
SAIC/Scripps Institution of Oceanography

ABSTRACT

Recent progress in the development of a physics-based numerical propagation model for the virtual transmission of acoustic communication signals in shallow water is presented. The ultimate objective is to provide for the prediction of the output of the quadrature detector (QD, an analog of the discrete Fourier transform) in a time-variant, doubly dispersive, shallow-water channel. Current model development concentrates on the modeling of the QD response in the presence of rough boundaries, reserving inclusion of effects caused by a time-varying sea surface or source/receiver motion to future implementations. Three-dimensional Gaussian beam tracing is used so that out-of-plane reflections from rough surfaces or sloping bathymetry can be adequately modeled. Model predictions of the impulse response for a real shallow-water environment are observed to agree well with measured impulse responses.

INTRODUCTION

Recent innovations in shallow-water undersea surveillance and exploration have necessitated the use of the underwater acoustic medium as the primary means of information exchange. Wireless communication between underwater stations separated in range by as much as 5 km with water depths as low as 10 m may be required. This task is complicated by the inherent spatiotemporal variability of this medium, and the complex nature of multipath arrival of energy for shallow-water environments [1]. Figure 1 illustrates some of the major processes that may affect underwater communication signals.

Multipath spread is caused by refraction governed by the sound-speed profile, reflections from boundaries, and scattering from inhomogeneities. Doppler spread arises from source/receiver motion or the motion of the reflectors and scatterers. These phenomena can significantly disperse and distort the signal as it propagates through the channel. A numerical propagation model that simulates these effects is desired for the systematic study of these phenomena. Such a model would also be a useful tool for environment-dependence assessment, performance prediction, and mission planning of communication systems.

This paper describes an approach for a physics-based model designed to simulate multipath spread and Doppler spread of high-frequency underwater acoustic communication signals. Multipath spread is handled via propagation through a refractive medium, as dictated by the sound-speed profile, and by the modeling of reflection and scattering from arbitrarily rough boundaries. Doppler spread is incorporated via the inclusion of source/receiver motion and sea-surface motion. While other phenomena (water mass fluctuations, scattering from water volume inhomogeneities or bubbles) can be responsible for signal distortions, it is believed that those included are the primary sources of spreading for

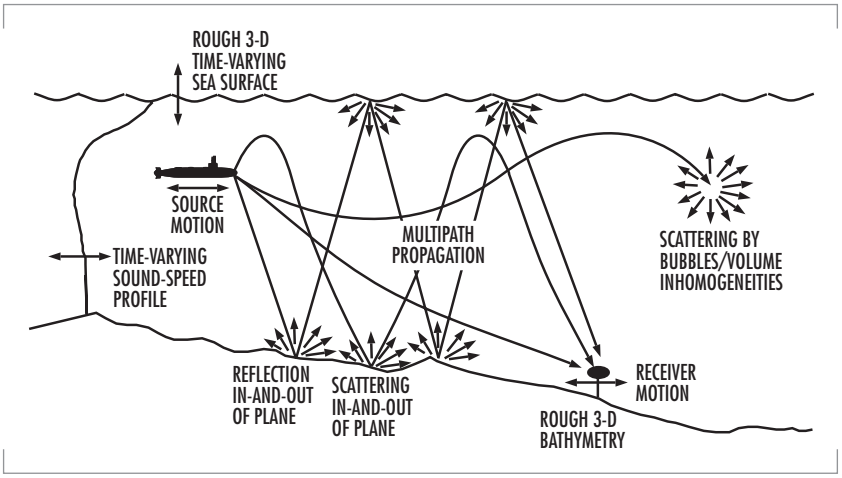

FIGURE 1. Some of the major processes affecting underwater acoustic communications signals.

many realistic problems. The present emphasis is on the modeling of propagation in a bounded refractive medium and the scattering from rough boundaries. The effects of a time-varying sea surface and source/receiver motion are reserved for future implementations.

The basic approach is to model the received output of the quadrature detector (QD) for a transmitted finite-duration constant-wavelength (CW) pulse. The QD is an analog version of the discrete Fourier transform, and provides a convenient means of obtaining the complex Fourier coefficients as a function of time for a finite-duration CW pulse. Because finite-duration CW pulses are common signals in communication schemes, the modeling of such signals is appropriate. However, a broadband QD response (for multiple CW pulses of different frequencies) can also be used to obtain a band-limited impulse response via Fourier synthesis, which is useful for the study of any arbitrary pulse signature.

The pulse is propagated by means of three-dimensional (3-D) Gaussian beams. The consideration of propagation in three dimensions is important because energy can be reflected or scattered in and out of the vertical plane containing both the source and receiver. The high frequencies of communication signals dictate the use of ray-based models over the less-efficient wave models or parabolic-equation approximations. Ray-based models also ensure proper handling of range-dependence and proper reflections from sloping boundaries. The only ray-based method practical for the 3-D problem is Gaussian beams, because the necessity of eigenray determination is eliminated. Ray theory without the use of Gaussian beams requires the determination of eigenrays (rays following paths connecting the source and receiver exactly), which is a formidable task in three dimensions. A dense fan of Gaussian microbeams allows direct modeling of scattering from arbitrarily rough surfaces.

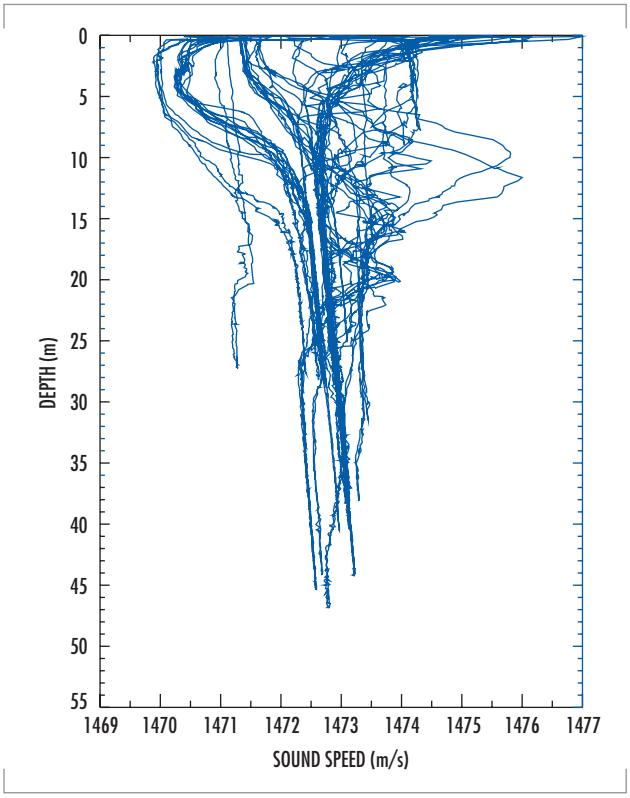

FIGURE 2. Composite of sound-speed profiles measured during the FRONT engineering test.

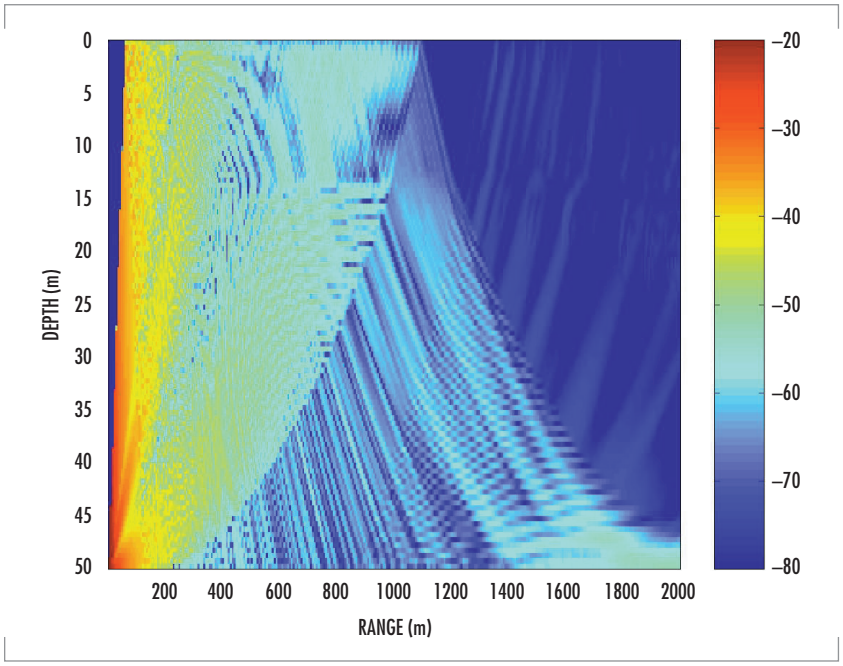

FIGURE 3. Predicted transmission loss during the FRONT engineering test.

EXAMPLE OF THE EFFECT OF PROPAGATION CONDITIONS ON COMMUNICATIONS

A compelling example of how ocean channel physics can affect underwater communications was

provided in engineering tests for the Front-Resolving Observatory with Networked Telemetry (FRONT) oceanographic network. The oceanographic conditions in the area are both interesting and complicated as fresh-river runoff interacts with the tides to generate a persistent front. Figure 2 shows a composite of sound-speed profiles measured at various locations over the duration of the experiment, demonstrating the great variability in the region. Within the upper 10 m of the water column, the channel varies between an upward-refracting (sound speed increases with depth) and downward-refracting (sound speed decreases with depth) channel. Figure 3 shows a transmission loss plot for a typical upward-refracting profile and a communications node (serving as the projector) located on the ocean bottom. This suggests that the influence of sea-surface roughness and time-variability will be greater when the channel is upward refracting.

During the course of the network deployment, there were periods with strong winds followed by relatively calm conditions as the wind speed plot shows in Figure 4A. As the wind speed increases, wave action drives up the ambient noise. At the same time, the roughness of the surface makes it a poor acoustic reflector, so the signal level drops. The combination of the two factors drives the signal-to-noise ratio (SNR) at the bottom-mounted receiver (Figure 4B). This, in turn, drives the overall modem performance as measured by the bit-error rate (Figure 4C). In summary, high winds caused network outages.

This is the simplest of mechanisms driving modem performance. Even with strong SNR, a modem that relies on a tap-delay line for adaptive equalization may fail if the multipath spread becomes too long. Similarly, a modem may fail to track Doppler changes, which is yet another dimension to the parameter space affecting modem performance.

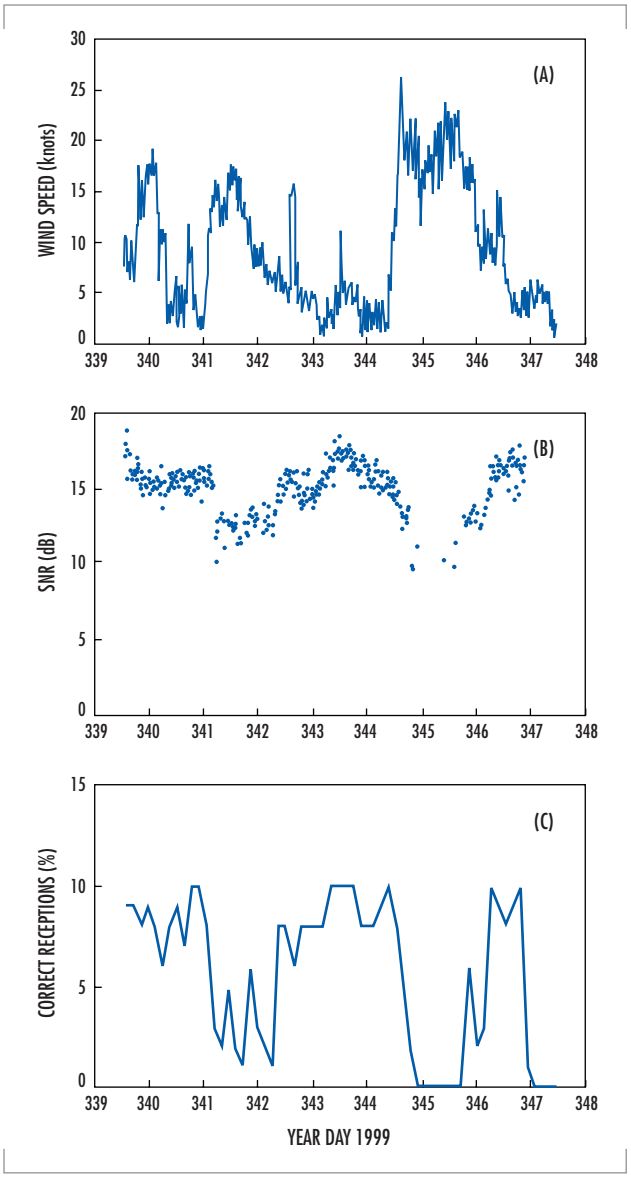

FIGURE 4. (A) During the FRONT network-engineering test, the wind speed varied considerably. (B) The wind speed affects the ambient noise and the surface reflectivity, which both drive the SNR at the receiver. (C) Variations in SNR, in turn, drive the performance of the modem.

3-D GAUSSIAN BEAM PROPAGATION MODEL

The 3-D Gaussian beam model is a modified version of that presented by Bucker [2]. For a specified sound-speed profile and seafloor, beams are traced from a source in three dimensions following the laws of ray acoustics and boundary interactions. Ray theory requires the determination of eigenrays, which can be computationally intensive, particularly in three dimensions. Determination of eigenrays is unnecessary in the Gaussian beam formulation. The sound field at a receiver is obtained by combining the coherent contributions of each beam as determined by the closest point of approach (CPA) of the beam path to the receiver. Consider an arbitrary beam path p that travels from a source S and passes close to a receiver X, as shown schematically in Figure 5A. The point x represents the CPA of the beam to the receiver and ρ is the CPA distance. The actual path length (arc length) from

S to x is designated S_x, and is shown linearized in Figure 5B. The pressure at the receiver X associated with this beam path is then given by

$$p = C_n B[\exp(-a\theta^2 + i\omega t)]/S_x, \quad (1)$$

where C_n is a normalization constant, a is an empirical constant, $\theta = \tan^{-1}(\rho / S_x)$, ω is the angular frequency, and t is the travel time to point x. A spherical wave-front correction equal to $(L\text{-}S_x)/c_x$, where $L^2=S_x^2+\rho^2$ and c_x is the sound speed at x, is included in the travel time t. B accounts for energy loss and phase shifts resulting from surface and bottom reflections. See [2] for a fuller explanation of the constants a and C_n.

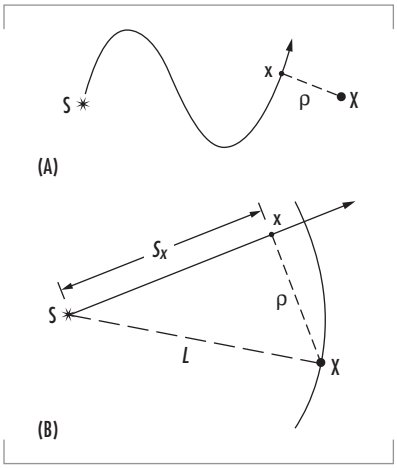

FIGURE 5. Geometry used to determine pressure contribution of a Gaussian beam at CPA to sensor X.

An important feature of the 3-D Gaussian beam model is that the bottom can be specified arbitrarily. Bottom depth data z are specified digitally by the user as a function of the horizontal coordinate directions x and y. Third-order smoothing polynomials are fitted to the bottom data in both directions so that the depth z and the unit normal $\tilde{n}$ can be determined for any arbitrary value of x and y (see appendix B of [2] for details). Bottom interactions are modeled via the specification of the reflection coefficient, or via the calculation of the reflection coefficient from specified geoacoustic parameters (sediment compressional and shear sound speed and attenuation and density). The bottom displacement technique of Zhang and Tindle [3] may also be used. Currently, only a semi-infinite representation for the bottom is implemented; this is sufficient for the high frequencies of interest in communication systems.

Arbitrary specification of the bottom depth implies that scattering problems may be handled directly and deterministically without the use of statistical techniques or approaches only applicable to particular classes of problems because of their underlying assumptions. Because the roughness can be arbitrarily specified, scattering effects are modeled by tracing a dense fan of very fine microbeams, which follow the physics of the interface interactions directly. By this means, problems at shallow grazing angles, such as self-shadowing effects, can be treated. In addition, using an arbitrary specification of bottom depth with 3-D Gaussian beams allows examination of environments possessing significant range-dependence.

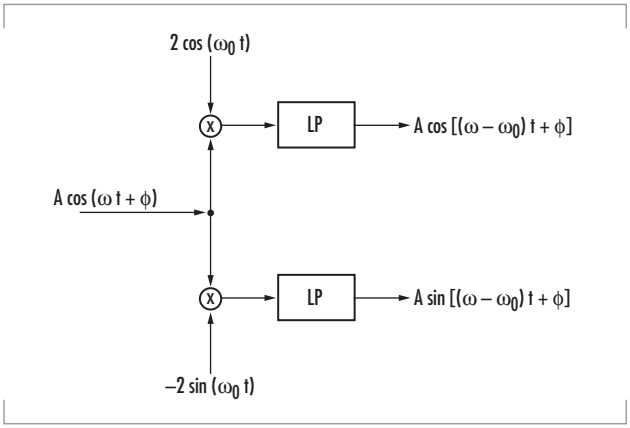

FIGURE 6. Quadrature detector algorithm for a continuous sinusoidal signal.

QUADRATURE DETECTOR RESPONSE

Assume that a continuous sinusoidal signal $A\cos(\omega t+\phi)$ arrives at a receiver, where ω is the frequency, t is the time, and ϕ is a phase shift associated with boundary interactions. If the signal is processed by a quadrature detector, as diagramed in Figure 6, the signal is split with one part being multiplied by $2\cos(\omega_0 t)$ and the other part being multiplied by $-2\sin(\omega_0 t)$. ω_0 is the reference frequency, which should be approximately equal to ω. Both parts are then passed through a low-pass filter to obtain the quadrature components $A\cos[(\omega-\omega_0)t+\phi]$ and $A\sin[(\omega-\omega_0)t+\phi]$, respectively. The complex output R_{QD} of the QD is then simply

$$R_{QD} = A\exp[i(\omega - \omega_0)t + \phi] , \quad (2)$$

This is basically an analog version of the discrete Fourier transform. If $\omega_0 \neq \omega$, R_{QD} will experience a rotation of $\omega-\omega_0$ radians per second.

Now assume that the incoming signal is a finite sinusoidal pulse of duration τ seconds and frequency ω. Assume also that the travel time from the source to the receiver along path p is t_p and that the time constant t_c (effective integration time) of the low-pass filters in the QD is τ seconds. For this case, R_{QD} is modulated by a triangle function $T(t)$ that is zero for $t<t_p$, increases linearly from zero to a value of unity at $t=t_p+\tau$, and then decreases linearly back to zero at $t=t_p+2\tau$. Therefore, the quadrature response for a beam travelling along path p is

$$R_{QD} = AT(t)\exp[i(\omega - \omega_0)t + \phi] , \qquad (3)$$

If the time constant t_c is larger than the pulse duration τ, R_{QD} remains at the value of the apex until $t>t_p+t_c$. In either case, R_{QD} still experiences the rotation $\omega - \omega_0$ if $\omega_0 \neq \omega$. The only way that ω_0 cannot equal ω in the above scenario is for a Doppler shift to have occurred somewhere along the path p. Therefore, source/receiver motion or sea-surface motion results in a rotation of R_{QD} for a path influenced by that motion. The total quadrature response of a received signal is therefore easily obtained by combining the quadrature responses of all paths contributing to the pressure at the receiver. This is facilitated via the use of the 3-D Gaussian beam model to propagate the energy. Closely spaced microbeams are launched from the source and traced through the refractive, bounded medium. Travel times, phase shifts associated with boundary reflections, and Doppler shifts associated with a moving source/receiver or with a moving sea surface are accumulated for each microbeam as it propagates. This information is then used with Eq. (3) to determine the QD response for each microbeam. A superposition of the QD response for all microbeams then provides the total QD response. If the pulse length is small, the QD response represents an estimate of the channel impulse response. The multipath structure resulting from refraction and the complex interactions of the many microbeams with the rough surface will combine to yield the effect of multipath spread on the QD impulse response. The Doppler shifts accumulated for each microbeam will combine to yield the effect of Doppler spread on the QD impulse response.

MODEL DEMONSTRATION

The environment selected for demonstrating the usefulness of the channel model was that of the SignalEx-99 experiment conducted in April 1999 in a shallow-water (~200 m) region, 6 km southwest of San Diego. Sponsored by the Office of Naval Research, SignalEx-99 was the first in a series of experiments intended to relate channel propagation characteristics to the performance of underwater acoustic communication systems. A detailed description of the experiment is provided by McDonald et al. [4].

The data considered here were linear frequency-modulated (LFM) chirps emitted/received from a source/receiver deployed at a depth of 30 m and source/receiver mounted 6.7 m above the seafloor. The source/receiver systems were telesonar test beds [5 and 6], autonomous units consisting of a single-board computer with a projector and a four-phone vertical line array. The 30-m test bed was deployed from a freely drifting ship, resulting in measurements as a function of time along a fairly constant track. The water depth at the receiver was 210 m, while the water depth decreased in a near linear fashion along the track to a depth of approximately 170 m at a range of 3.8 km from the receiver. Transmissions were made in both directions between the two test beds.

Figure 7 shows the bathymetry and track of the drifting source. Northerly winds caused the ship to drift from a range of about 0 to 4 km (Drift 1). As the range was becoming large and the ship began drifting off the isobath, the ship was repositioned back at a range of about 2 km and allowed to drift again (Drift 2). This conveniently provided a look at the consistency of the Drift 1 results. Once again, the ship drifted to a range of about 6.5 km and was repositioned and moored at a range of 4.75 km providing a look at the stability of the signaling schemes with fixed source-receiver geometry.

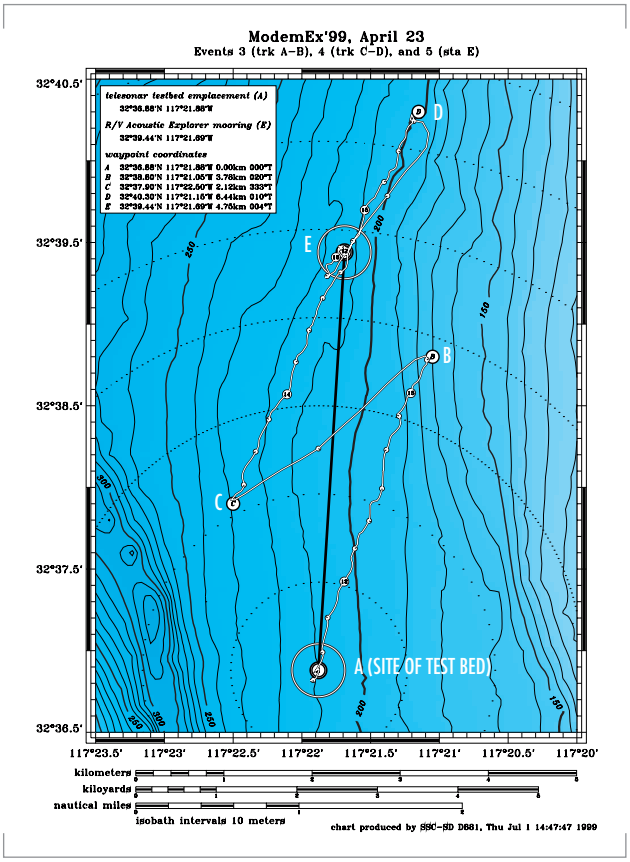

FIGURE 7. Bathymetry and source track for SignalEx-99 experiment. Drift 1 is from A to B (source range = 0 to 3.8 km). Drift 2 is from C to D (source range = 2.1 to 6.5 km). The moored station is at E (source range = 4.75 km).

Figure 8 shows a typical sound-speed profile measured during the SignalEx-99 experiment. The profile is strongly downward refracting with approximately a 20-m mixed layer at the surface and a slight duct forming near the bottom. It has been determined previously [7] that the bottom in this region may be treated as a fluid with a compressional sound speed of 1572.37 m/s, a compressional attenuation of 0.20 dB/kmHz, and a density of 1.76 g/cm^3.

The LFM chirps were transmitted sweeping the 8- to 16-kHz band over a 1-second period. Sixteen chirps were transmitted in 10-minute time frames over a 5-hour period. The direction of the transmission was switched for consecutive 10-minute periods. Theoretically, the impulse response is a combination of these chirps delayed in time according to their path length and attenuated according to volume absorption and reflection loss at the boundaries. The impulse response can be estimated experimentally by correlating the received pulses with a replica of the original transmitted pulse. This produces a sequence of impulses corresponding to each echo in the received waveform, thereby providing a visualization of the impulse response. Figure 9 shows the result of performing this correlation as a function of time. The variation in the multipath structure throughout the experiment is clearly observed. Because absolute times were not available, the first significant peak in each reception was detected and used to provide a leading-edge alignment. Note also that this plot is a composite of the transmissions that alternated between the ship and bottom-mounted test bed.

Figure 10 compares the measured impulse response at a time of day of 12.5 hours (ping number 34) to a simluated response obtained via the 3-D Gaussian beam, quadrature detector model for the same source-receiver configuration. The source range at this time was 2.2 km. The simulation was performed assuming a flat bottom at a water depth of 210 m, and ignoring the effects of rough-surface scattering and time-variability. The measured impulse response has been normalized relative to the maximum, and the arbitrary time scale has been shifted to facilitate comparison with the modeled result. Note that the predicted arrivals agree well with the measured arrivals, indicating that refraction and reflection

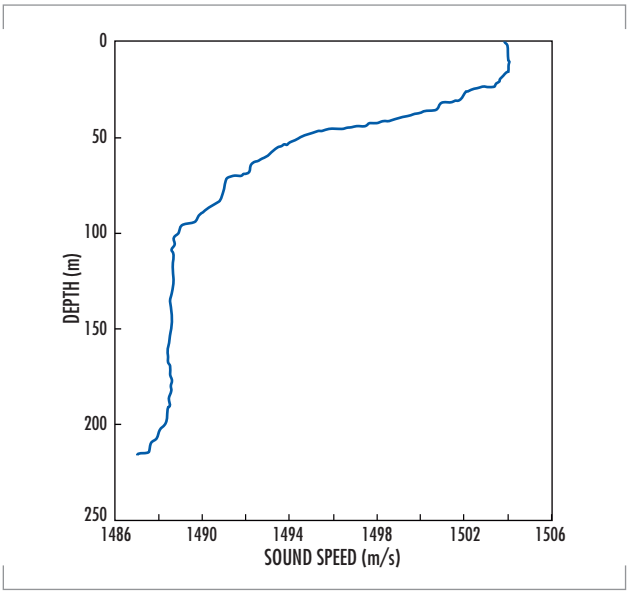

FIGURE 8. Typical sound-speed profile measured during SignalEx-99 experiment.

from boundaries are well modeled. Time dicrepancies between arrival paths may be caused by the neglect of the varying bathymetry or errors in the assumed sound-speed profile. The higher resolution of the model results indicates that the first arrival is actually a combination of several arrivals: namely, the direct path, the one-bottom-reflected path, the one-surface-reflected path, and the one-surface-reflected/one-bottom-reflected path. Likewise, the later arrivals are actually a combination of several higher order paths. Note also that the data exhibits a gradual rolloff after the arrival of the pulses, suggesting a reverberant environment. The likely cause of this behavior is the scattering of energy in three dimensions caused by the interaction of rays with the boundaries. Future work will attempt to model these interactions.

Future developments of the model will focus on determining how scattering from rough surfaces, source/receiver motion, and sea-surface motion will influence these responses.

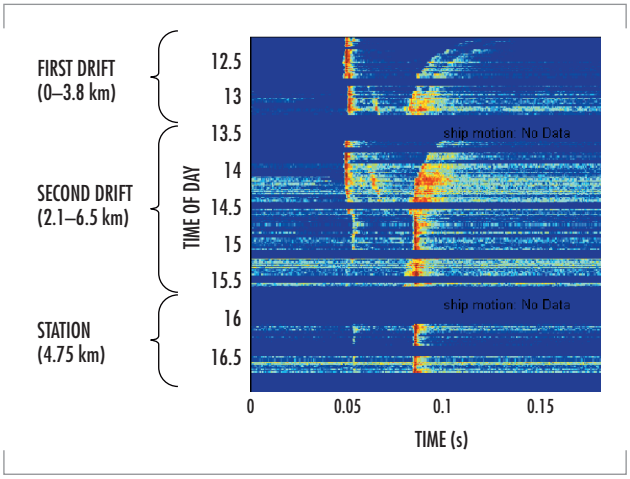

FIGURE 9. Replica correlogram from chirps during SignalEx-99 experiment.

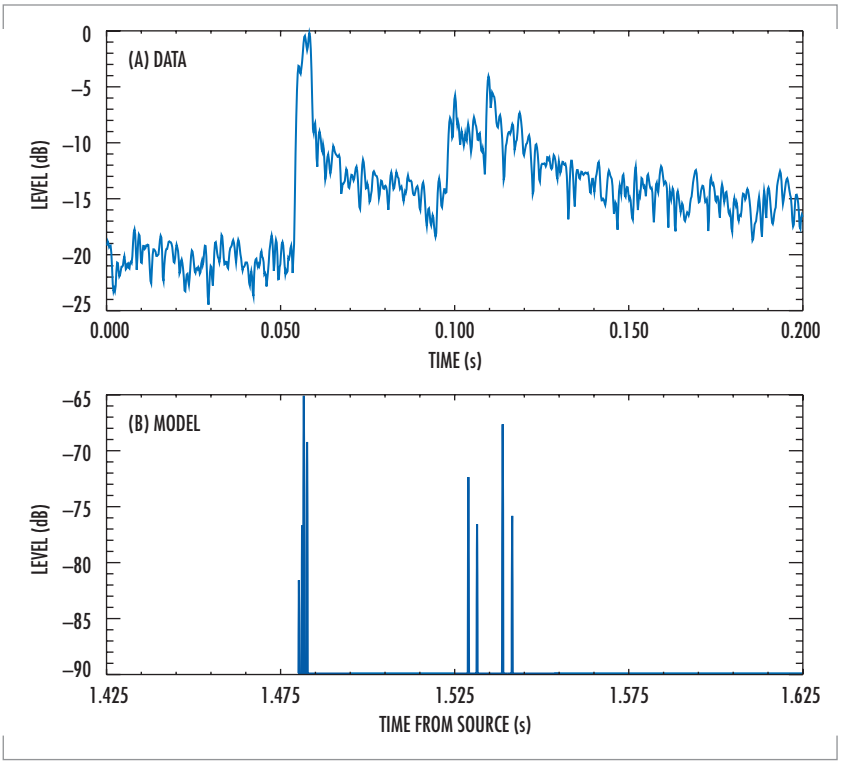

FIGURE 10. Comparison between (A) measured and (B) modeled impulse responses. Time of day = 12.5 hours. Source range = 2.2 km.

MODELING SURFACE AND BOTTOM SCATTER

Scattering from rough boundaries produces losses in signal energy. These losses are two-fold. First, scatter converts energy to higher angles eventually allowing it to penetrate the bottom where it is absorbed. Second, it destroys the coherence of the wave producing what might be termed an apparent loss. For instance, a moving surface will stretch and compress a sinewave reflected from it. If the reflected energy is detected by a matched-filter expecting a perfect sinewave, it will see a reduced power level. This discussion applies, for instance, to a single tone in an M-ary Frequency-Shift Keying (MFSK) signaling scheme, where the tone is detected by a filter bank. If we have a rough bottom with a static geometry, this loss of coherence does not occur. However, if the source or receiver moves, we have a dynamic situation similar to the surface loss just described.

In round numbers, a typical communications carrier gives a wavelength around 10 cm. A classical measure of the role of roughness—the Rayleigh roughness parameter—is the ratio of the roughness to the wavelength (or more precisely, the vertical component of the wavelength). As this number becomes close to unity, losses per bounce become large, perhaps 10 dB, and many of the standard scatter models that assume small roughness fail. The point of this discussion is that 10-cm roughness is easily attained on both surface and bottom boundaries in real environments, implying large boundary losses. Furthermore, the roughness is typically not known to within 10 cm, implying large uncertainty in those same losses and in the resulting transmission loss.

Finally, the actual scatter mechanisms are complicated. In some cases, the air–water interface is the scatterer. In other cases, the bubbles below are likely to be dominant. Similarly, at the ocean bottom, scatter can occur at the interface or by inhomogeneities just below the interface (though not too far below because volume attenuation limits the sediment penetration significantly).

As a first step toward modeling scattering effects, we assume that the boundary roughness dominates the problem, and concentrate first on the bottom roughness. A common approach [8] to characterize this roughness is to use the spatial power spectral density, i.e., the power spectrum of the bottom roughness. Various forms may be used; however, one popular choice is $\Phi(k) \propto k^{-b}$, where b is a measured parameter for the particular site. Suggested values for b are given in [8] along with the RMS roughness that defines the overall amplitude of the spectrum.

Given the spatial power spectral density, we can construct individual realizations of the bottom by using a standard technique. In particular, we convert the power spectrum to an amplitude spectrum by taking its square root. We discretely sample the amplitude and then introduce a random phase. Finally, we do a fast Fourier transform (FFT) to produce and add in the mean depth to obtain a single realization of the bottom. In equations:

$$D(r) = \int A(k) e^{\theta} e^{ikr} dk \qquad (4)$$

where $A(k) = \sqrt{\Phi(k)}$ and $\Phi(k) = 5.5 \times 10^{-5} k^{-2.25}$
is the spatial power density spectrum for a particular area.

As a specific example, Figure 11 shows a single realization of the bottom depth using the above described power spectrum. Figure 12 compares the

predicted transmission loss for the SignalEx-99 environment using this rough bottom (Figure 12A) with that predicted using a smooth bottom (Figure 12B). The transmission loss calculation was done using the BELLHOP ray/beam model [9], which is a two-dimensional (2-D) version of the 3-D Gaussian beam model. The prediction is for the case of a test bed deployed on the seafloor. Note the fill-in of the shadow zone near the surface at a range of 2 km. There are also changes in the Lloyd-mirror pattern emanating from the source.

The root-mean-square (RMS) height used here is 0.23 m, which is fairly low. There will also be surface scatter that may also be expected to have a larger RMS roughness.

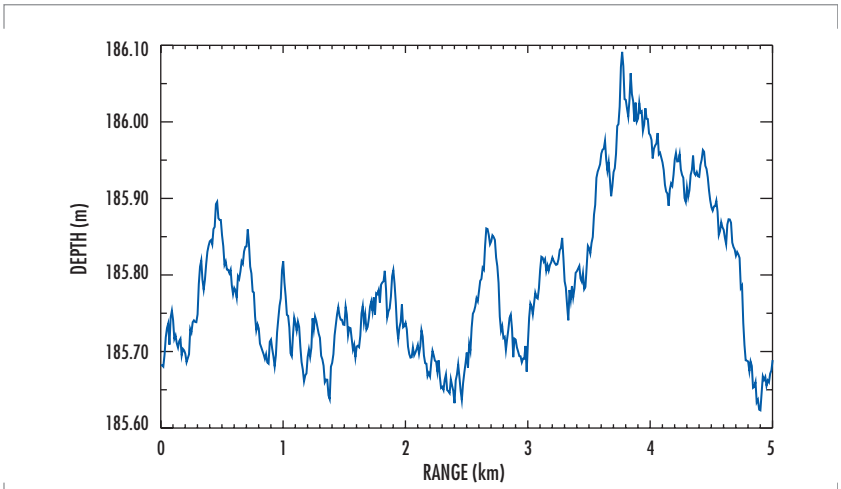

FIGURE 11. Single realization of the bottom depth using a power-law spectrum.

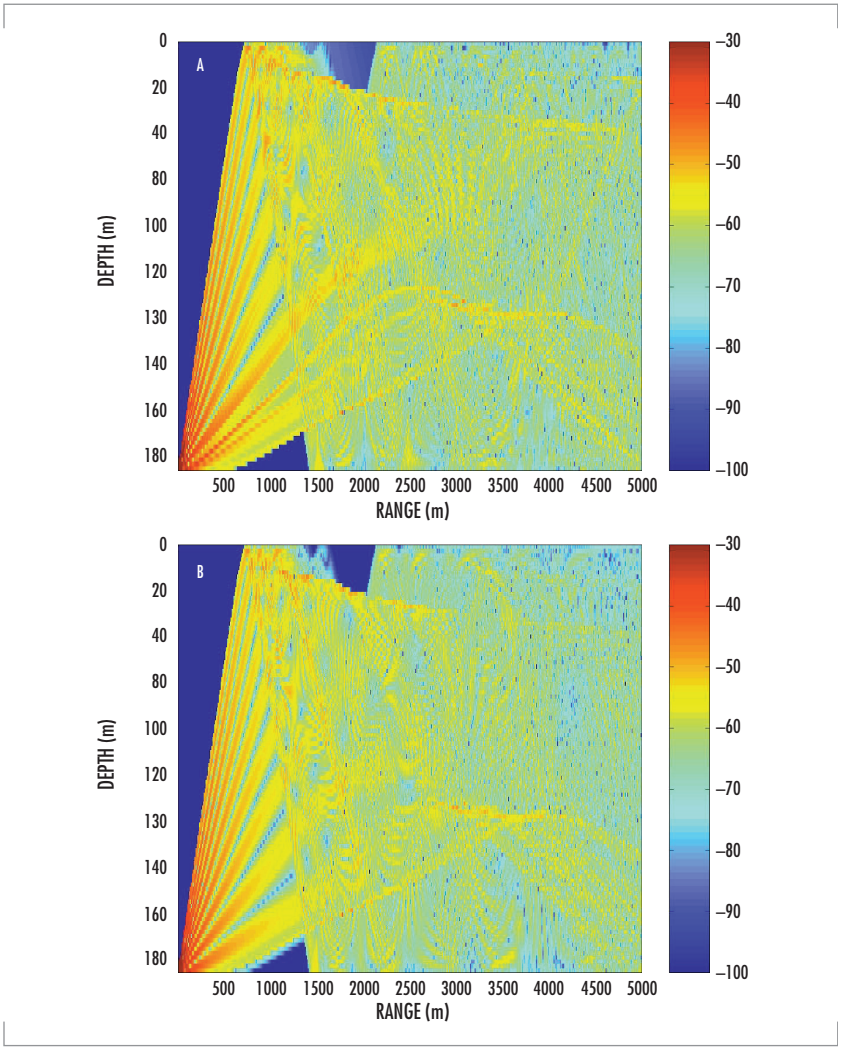

FIGURE 12. Comparison of predicted transmission loss for the SignalEx-99 environment (A) using the rough bottom in Figure 11, and (B) using a smooth bottom. Source is near the seafloor.

SUMMARY AND FUTURE APPLICATIONS

The channel model outlined in this paper is being developed to aid in the analysis of future underwater acoustic communication systems. The modeling of the QD response via the use of 3-D Gaussian beams enables the inclusion of physical phenomena known to influence such systems in a computationally efficient manner. The model will provide a useful tool for examining the effect of multipath and Doppler spread on the performance of these systems. Because it is designed for use with finite-duration CW pulses, the model can be used directly for the analysis of MFSK systems. Otherwise, the model can also be run for multiple frequencies to obtain a band-limited impulse response via Fourier synthesis.

The following future work is planned. An analytical model will be implemented for a sinusoidally

corrugated interface and used as a benchmark solution to validate the above ray/beam results for scatter from a rough surface. The 2-D scattering approach will be expanded to provide 3-D scattering for inclusion in the 3-D Gaussian beam quadrature detector model. The importance of 3-D scattering effects on the impulse response will then be studied. These tasks are geared to evaluating the mean energy level in a situation where the processing time is short enough that a "frozen ocean" model is appropriate. Once this is accomplished, a time-varying sea surface will be implemented.

Work is underway to use the model to infer channel characteristics such as coherence time, coherence bandwidth, multipath spread, and Doppler spread. It will also be used as part of a statistically governed Markov process to produce a time-dependent simulation.

ACKNOWLEDGMENTS

The Office of Naval Research (ONR) via the SSC San Diego In-house Laboratory Independent Research (ILIR) Program sponsored this work. The SignalEx-99 experiment was sponsored by ONR 322OM via the Telesonar Signaling Measurements Project. The FRONT program is sponsored by the National Oceanographic Partnership Program (NOPP). The authors also thank Robert Creber and Christopher Fletcher for their help in obtaining experimental data.

AUTHORS

Homer Bucker
Ph.D. in Physics, University of Oklahoma, 1962
Current Research: Matched-field tracking; underwater acoustic propagation modeling using three-dimensional Gaussian beams.

Vincent K. McDonald
BS in Mathematics, San Diego State University, 1988
Current Research: Underwater acoustic communications research; underwater surveillance system design.

Joseph A. Rice
MS in Electrical Engineering, University of California at San Diego, 1990
Current Research: Ocean sound propagation; sonar systems analysis; undersea wireless networks.

Michael B. Porter
Ph.D. in Engineering Sciences and Applied Mathematics, Northwestern University, 1984
Current Research: Array signal processing; acoustic communications; wave propagation.

REFERENCES

1. Rice, J. A. 1997. "Acoustic Signal Dispersion and Distortion by Shallow Undersea Transmission Channels," *Proceedings of the NATO SACLANT Undersea Research Centre Conference on High-Frequency Acoustics in Shallow Water*, pp. 425–442.
2. Bucker, H. P. 1994. "A Simple 3-D Gaussian Beam Sound Propagation Model for Shallow Water," *Journal of Acoustical Society of America*, vol. 95, no. 5, pp. 2437–2440.

3. Zhang, Z. Y. and C. T. Tindle. 1993. "Complex Effective Depth of the Ocean Bottom," *Journal of Acoustical Society of America*, vol. 93, no. 1, pp. 205–213.
4. McDonald, V. K., J. A. Rice, M. B. Porter and P. A. Baxley. 1999. "Performance Measurements of a Diverse Collection of Undersea Acoustic Communication Signals," *Proceedings of IEEE Oceans '99 Conference*, 13 to 16 September, Seattle, WA.
5. McDonald, V. K., and J. A. Rice. 1999. "Telesonar Testbed—Advances in Undersea Wireless Communications," *Sea Technology*, vol. 40, no. 2, pp. 17–23.
6. McDonald, V. K., J. A. Rice, and C. L. Fletcher. 1998. "An Underwater Communication Testbed for Telesonar RDT&E," *Proceedings of MTS Ocean Community Conference '98*, 16 to 19 November, Baltimore, MD.
7. Baxley, P. A., N. O. Booth, and W. S. Hodgkiss. 2000. "Matched-Field Replica Model Optimization and Bottom Property Inversion in Shallow Water," *Journal of Acoustical Society of America*, vol. 107, no. 3, pp. 1301–1323.
8. Medwin, H. and C. S. Clay. 1998. *Fundamentals of Acoustical Oceanography*, Academic Press, San Diego, CA.
9. Porter, M. B. and Y-C Liu. 1994. "Finite-Element Ray Tracing," *Theoretical and Computational Acoustics*, (D. Lee and M. H. Schultz, eds.) World Scientific Publishing Company, River Edge, NJ, vol. 2, pp. 947–956.

❖

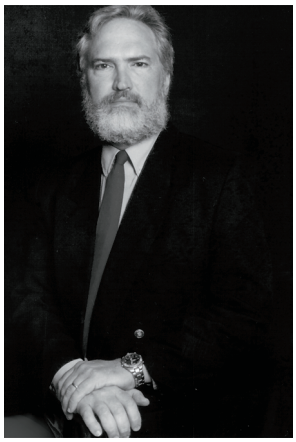

Paul Baxley
MS in Oceanography, Scripps Institution of Oceanography, University of California at San Diego, 1998
Current Research: Underwater acoustic communication modeling; matched-field source localization and tracking; seafloor geoacoustic property inversion.